

quence of continent-continent collisions between large plates that are strongly coupled to mantle flow, and may thus provide a means of linking major tectonic events that have occurred throughout Earth's geologic history.

REFERENCES AND NOTES

- R. M. Russo and P. G. Silver, *Science* **263**, 1105 (1994).
- , *Geology* **24**, 511 (1996).
- S. Uyeda and H. Kanamori, *J. Geophys. Res.* **84**, 1049 (1979).
- T. Sempere *et al.*, *Geology* **18**, 946 (1990).
- P. Shaw and S. C. Cande, *J. Geophys. Res.* **95**, 2625 (1990).
- J. M. O'Connor and R. A. Duncan, *ibid.*, p. 17475.
- J. M. O'Connor and A. P. le Roex, *Earth Planet. Sci. Lett.* **113**, 343 (1992).
- Supporting evidence for this reduction in the Af velocity was summarized by K. Burke [S. Afr. J. Geol. **99**, 341 (1996)].
- K. J. Hsu, *Geol. Soc. Am. Spec. Pub.* **45**, 421 (1989).
- J. Dercourt, L. E. Ricou, B. Vrielynck, Eds., *Atlas Tethys Paleoenvironmental Maps* (Gauthier-Villars, Paris, 1993).
- A. E. Gripp and R. G. Gordon, *Geophys. Res. Lett.* **17**, 1109 (1990).
- P. R. Stoddard and D. Abbott, *J. Geophys. Res.* **101**, 5425 (1996).
- There are several lines of evidence supporting the notion that SA is coupled to general mantle circulation. First, the only other potentially significant driving force, ridge-push, does not change on sufficiently short time scales to cause such a rapid change in plate motion. The change must be caused by changes in the tractions at the plate boundary or basal tractions. There is no evidence for a decrease in boundary resistance forces or increase in boundary driving forces, so the only alternative is a change in the basal traction (that could take the form of basal shear tractions or possibly horizontal normal tractions applied to the sides of deep continental roots). Other lines of evidence include: the apparent absence of an asthenospheric decoupling zone beneath continental plates in general [P. G. Silver, *Annu. Rev. Earth Planet. Sci.* **24**, 385 (1996)] and South America in particular [D. E. James and M. Assumpção, *Geophys. J. Int.* **126**, 1 (1996)], as inferred from seismic anisotropy, and the suggestion, from seismic tomography of coherent translation of the SA plate and upper mantle over the last 130 My [J. C. VanDecar, D. E. James, M. Assumpção, *Nature* **378**, 25 (1995)]. If SA is coupled to mantle circulation, it is reasonable to suppose that the other plates of the Atlantic basin, particularly Africa, are similarly coupled (2). For a general discussion of coupling of plate motions to mantle circulation, see C. Lithgow-Bertelloni and M. A. Richards, *Rev. Geophys.*, in press.
- It is unlikely for there to be any other way for stress to be transmitted from Af to SA. If transmitted through the plates themselves (acting as a stress guide), the stress would have to cross the ridge, where plates are thinnest, leading to a severe disruption in the spreading process, which is not observed.
- C. Lithgow-Bertelloni and M. A. Richards, *Geophys. Res. Lett.* **22**, 1317 (1995). We used a density heterogeneity model based on the 200 My of subduction preceding 25 Ma and on oceanic lithospheric ages consistent with the plate boundaries and age of the stage. The viscosity structure used in the calculation (a lower mantle 50 times more viscous than the upper mantle) represents the value obtained from a fit to the geoid, assuming a present-day density heterogeneity field based on subduction history. The absolute viscosity was fixed at 10^{21} Pa·s, a value compatible with inferences from post-glacial rebound.
- By allowing Af and Eu to act as one plate, we are implicitly allowing infinite compressional stresses to develop at the plate boundary between them, maximizing the effect of the collision. The size of the colliding plates is crucial for the collision to have any effect on the general mantle circulation. This approach was attempted previously (17) as a way of testing the influence of the India/Eurasia collision on the Pacific Plate, although no change in plate motion was found.
- M. Richards and C. Lithgow-Bertelloni, *Earth Planet. Sci. Lett.* **137**, 19 (1996).
- These are estimated from balanced cross sections, which range from 100 to 200 km: F. Mégard, *J. Geol. Soc. London* **129**, 893 (1984); B. M. Sheffels, *Geology* **18**, 812 (1990); R. W. Allmendinger *et al.*, *Tectonics* **2**, 1 (1983); R. W. Allmendinger *et al.*, *ibid.* **9**, 789 (1990); P. Baby *et al.*, *ibid.* **11**, 523 (1992).
- L. Leffler *et al.*, *Geophys. Res. Lett.*, **24**, 1031 (1997); E. Norabuena *et al.*, *Science*, in press.
- Described by M. A. Richards and D. C. Engebretson [*Eos Trans. Am. Geophys. Union* **75**, 63 (1994)] for Pacific-Farallon motions at the time of the formation of the bend in the Hawaii-Emperor sea mount chain. S. Zhong and M. Gurnis [*Nature* **383**, 245 (1996)] showed that transforms guide plate motions in mantle convection models with realistic faults and plates.
- J. Mammerickx and D. Sandwell, *J. Geophys. Res.* **91**, 1975 (1986).
- This estimate is based on the assumption that SA's northward motion is primarily driven by basal shear and that the ridge-transform offsets have become the dominant resistive force once SA's northward motion has ceased.
- T. H. Dixon and A. Mao, *Geophys. Res. Lett.* **24**, 535 (1997).
- S. Stein, H. J. Melosh, J. B. Minster, *Earth Planet. Sci. Lett.* **36**, 51 (1977).
- J. G. Schilling, *Nature* **352**, 397 (1991).
- N. Oskarsson, S. Steinthorsson, G. E. Sigvaldason, *J. Geophys. Res.* **90**, 10011 (1985).
- W. J. Morgan, *Am. Assoc. Pet. Geol. Bull.* **56**, 203 (1972).
- J. Madeira and A. Ribeiro, *Tectonophysics* **184**, 405 (1990).
- E. Widom, R. W. Carlson, J. B. Gill, H. U. Schmincke, *Chem. Geol.*, in preparation.
- The New England hot spot in the Great Meteor-Atlantis seamounts [R. A. Duncan, *J. Geophys. Res.* **89**, 9980 (1984); B. E. Tucholke and N. C. Smoot, *ibid.* **95**, 17555 (1990)], which also lie a few hundred kilometers east of the adjacent MAR. Further south, isotopically distinct Sierra Leone, Circe, Shona, and Discovery mantle plumes have been observed in a similar eastward-displaced position relative to the local MAR [C. J. H. Hartnady and A. P. leRoex, *Earth Planet. Sci. Lett.* **75** (1985); J. G. Schilling *et al.*, *J. Geophys. Res.* **99**, 12005 (1994); J. Douglass, J. G. Schilling, R. H. Kingsley, C. Small, *Geophys. Res. Lett.* **22**, 2893 (1995)]. Although the motion histories of these hot spots are poorly known compared to that of Iceland or Tristan da Cunha, the regular distribution of near-MAR hot spots on the east side of the ridge is compatible with westward drift of the MAR relative to Atlantic basin hot spots since at least 30 Ma.
- D. T. Sandwell and W. H. F. Smith, *J. Geophys. Res.*, in press.
- We thank W. Smith for providing us with a custom version of Atlantic basin gravity anomalies; S. Solomon, C. DeLima, S. Stein, P. Lundgren, C. Bina, A. Nicolas, and A. le Roex for stimulating discussions; S. Sacks for South American GPS data before publication; J. Dunlap for manuscript preparation; and M. Acierno and S. Keiser for computer support. We used GMT (P. Wessel and W. Smith) to make many figures in this report. Supported by NSF grant EAR 93-16457 (P.G.S. and R.R.), by an NSF-NATO Fellowship (R.R.), by an NSF postdoctoral fellowship (C.L.-B.) and by the Carnegie Institution of Washington (P.G.S. and C.L.-B.).

3 February 1997; accepted 24 November 1997

Footwall Refrigeration Along a Detachment Fault: Implications for the Thermal Evolution of Core Complexes

Jean Morrison* and J. Lawford Anderson

Oxygen isotope compositions of epidote and quartz from chloritic breccias that underlie the detachment fault in the metamorphic core complex of the Whipple Mountains yielded quartz-epidote fractionations that range from 4.1 to 6.4 per mil and increase systematically toward the fault. These fractionations give mean temperatures that decrease from $\sim 432^\circ\text{C}$ at 50 meters below the fault to $\sim 350^\circ\text{C}$ at 12 meters below the fault. This extreme thermal gradient of 82°C over 38 meters (2160°C per kilometer) is best explained by advective heat extraction by means of circulating surface-derived fluids. Models of lithospheric extension consider only conductive cooling resulting from tectonic denudation and thus require revision to include fluid-induced fault-zone refrigeration.

Metamorphic core complexes of the western North American cordillera formed during pronounced Cenozoic crustal extension at the lithospheric scale. Core complexes are characterized by regionally extensive, low-angle detachment faults that accom-

modate large, lateral displacements of the crust (1–3). An accurate and quantitative understanding of the nature of movement along detachment faults is essential in developing realistic models of lithospheric extension. However, many aspects of detachment fault systems, including the determination of whether they initiate and slip at low angles ($<30^\circ$), the rates at which they slip, and the role that fluids play in the

Department of Earth Sciences, University of Southern California, Los Angeles, CA 90089-0740, USA.

*To whom correspondence should be addressed.

mechanics of slip, remain controversial (4–13). Many of the important quantitative constraints on detachment-related processes are based on thermal characteristics of the footwall. Fission track and $^{40}\text{Ar}/^{39}\text{Ar}$ spectra have been used to determine footwall cooling histories and infer uplift rates (14–17). In addition, the initial fault dip can be inferred if the predetachment geothermal gradient can be reliably established (18). Using laser-based microanalytical techniques, we have measured $\delta^{18}\text{O}$ values of spatially related quartz and epidote grains in chloritic breccias from the Whipple Mountains to determine temperatures of detachment fault-related processes (Table 1). The data reveal an extreme negative thermal gradient within ~ 50 m of the detachment fault. This gradient has important implications for understanding the thermal characteristics of the footwall and thus the evolution of the core complex.

The Whipple Mountains metamorphic core complex of southeastern California contains the structural and petrologic features that characterize most cordilleran complexes and is one of the most well studied. Brittle deformation and fluid circulation that accompany detachment faulting have transformed footwall gneisses into aphanitic cataclasite at the fault surface and chloritic breccia below; the breccias exhibit

grain size reduction but are not penetratively sheared. Aphanitic and silicified cataclasite microbreccia varying from 2 to 25 cm thick underlies the detachment fault surface and overlies chloritic breccias that vary from a few meters up to 300 m thick (19). In Bowman's Wash ($34^\circ, 17'\text{N}$, $114^\circ, 17'\text{W}$), the detachment fault cuts a leucocratic biotite tonalite of the lower-plate Cretaceous Whipple Wash suite. We collected samples from this altered rock unit along a single traverse at distances below the fault of ~ 50 m (90-WP-14), 40 m (90-WP-13), 25 m (90-WP-12), 12 m (90-WP-11), and 2 m (90-WP-10) and at the fault surface (90-WP-9); 90-WP-10 and -9 are microbreccia samples. As a result of hydrothermal alteration and brittle deformation, the tonalite contains chlorite, epidote, muscovite (sericite), quartz, plagioclase, sphene, calcite, hematite, and sometimes biotite. In these samples, sericitic alteration of plagioclase becomes increasingly fine-grained and more abundant, biotite is replaced by chlorite, and neoblastic chlorite and epidote increase in abundance toward the fault.

We analyzed five discrete quartz-epidote pairs from each of the four chloritic breccia samples (20). Two methods were used to extract mineral pairs. Either adjacent epidote and quartz grains were picked directly

from strips ~ 1 mm wide cut from slabs ~ 0.5 mm thick or grains were picked from ~ 0.5 cm^3 crushed volumes. Because fine-scale textural relations are lost in this latter process, two grains of epidote or quartz were usually extracted. The two $\delta^{18}\text{O}$ values were averaged, and the mean values are reported in Table 1. Individual epidote $\delta^{18}\text{O}$ values from ~ 0.5 cm^3 crushed volumes differed by an average of 0.47 ± 0.21 per mil ($n = 12$), and quartz $\delta^{18}\text{O}$ values differed by an average of 0.39 ± 0.24 per mil ($n = 4$).

Epidote (Ep) and quartz (Qtz) $\delta^{18}\text{O}$ values form a generally linear array with a steep positive slope (Fig. 1). Temperatures corresponding to lines of constant $\Delta_{\text{Qtz-Ep}}$ ($=\delta^{18}\text{O}_{\text{Qtz}} - \delta^{18}\text{O}_{\text{Ep}}$) were calculated using the calibration of Matthews (21) for pure epidote and quartz. Similar trends for coexisting feldspar and quartz in granitic rocks are often interpreted to reflect disequilibrium caused by partial exchange with a low- $\delta^{18}\text{O}$ fluid because feldspar exchanges more rapidly with the fluid than does quartz (22). Because both epidote and quartz were likely present in the biotite tonalite before brecciation and hydrothermal alteration, it is important to assess whether the data reflect disequilibrium processes. Unlike feldspar, however, epidote is a relatively dense (3.38 to 3.49 g/cm^3) Ca-, Al-, Fe-bearing silicate, which, by analogy with similar minerals such as garnet, should exchange more slowly than quartz. Thus, partial or disequilibrium exchange with a low $\delta^{18}\text{O}$ fluid would produce a flat trajectory on Fig. 1 because quartz $\delta^{18}\text{O}$ values would be most affected by exchange with the fluid. The steep slope of the array is, therefore, inconsistent with disequilibrium exchange. We interpret observed systematic variations (Fig. 1) to reflect equilibrium exchange with a fluid at variable temperatures. We interpret the sympathetic variation in

Table 1. Oxygen isotopic compositions of chloritic breccia samples from the Whipple Mountains. The isotopic ratio is calculated as:

$$\delta^{18}\text{O} = \left[\frac{(^{18}\text{O}/^{16}\text{O})_{\text{sample}}}{(^{18}\text{O}/^{16}\text{O})_{\text{SMOW}}} - 1 \right] \times 10^3$$

where SMOW is standard mean ocean water.

Sample	Quartz $\delta^{18}\text{O}$ (per mil)	Epidote $\delta^{18}\text{O}$ (per mil)	$\Delta_{\text{Qtz-Ep}}$ (per mil)	Temperature* ($^\circ\text{C}$)
90-WP-14-1†	10.03	5.45	4.58	427
90-WP-14-2†	9.52	4.23	5.29	379
90-WP-14-3†	9.70	5.29	4.41	441
90-WP-14-4	9.20	4.83	4.37	444
90-WP-14-5	8.83	4.76	4.07	470
90-WP-13-1†	9.37			
90-WP-13-2†	8.66	3.21	5.45	369
90-WP-13-3†	8.71	2.88	5.83	348
90-WP-13-4	9.07	5.49	3.58	519
90-WP-13-5	9.49	4.70	4.79	412
90-WP-13-6	9.04	4.27	4.77	413
90-WP-12-1	9.39	3.95	5.44	370
90-WP-12-2	9.10	4.30	4.80	411
90-WP-12-3	9.22	4.17	5.05	394
90-WP-12-4	8.93	4.31	4.62	424
90-WP-12-5	9.70	4.39	5.31	377
90-WP-11-1	8.79	2.66	6.13	332
90-WP-11-2	8.29	2.82	5.47	368
90-WP-11-3	8.58	2.21	6.37	321
90-WP-11-4	8.73	2.75	5.98	340
90-WP-11-5	8.37	3.28	5.09	391
90-WP-10	7.90			
90-WP-9	8.30‡			

*Calculated on the basis of the calibration of Matthews (21). †Grains removed from strips; all other grains were picked from ~ 0.5 cm^3 of crushed material. ‡Whole-rock $\delta^{18}\text{O}$ value.

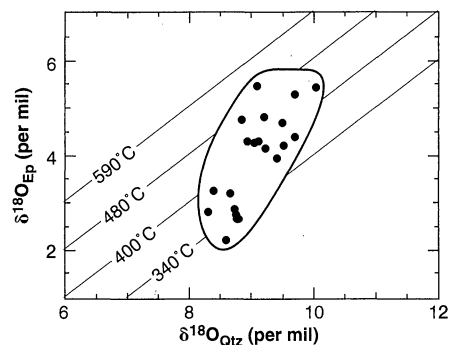


Fig. 1. Quartz $\delta^{18}\text{O}$ versus epidote $\delta^{18}\text{O}$ values for coexisting pairs from chloritic breccia samples. Temperatures corresponding to lines of constant $\Delta_{\text{Qtz-Ep}}$ were calculated using Matthews (21). The data are interpreted to indicate equilibration between quartz and epidote at temperatures ranging from $\sim 520^\circ$ down to $\sim 320^\circ\text{C}$.

both quartz and epidote $\delta^{18}\text{O}$ values (Fig. 1) as an indication that they equilibrated during cataclastic deformation and fluid infiltration and that equilibration occurred locally between adjacent grains.

Mean $\Delta_{\text{Qtz-Ep}}$ values increased toward the detachment fault from 4.54 ± 0.46 per mil at 50 m below the fault to 5.81 ± 0.52 per mil at 12 m (Fig. 2). The corresponding mean temperatures decrease from $432^\circ \pm 34^\circ\text{C}$ at 50 m below the fault to $350^\circ \pm 29^\circ\text{C}$ at 12 m. This decrease in temperature is consistent with mineralogic variations including a decrease in grain size of sericitic alteration and progressive obliteration of the original igneous textures.

Temperatures of predetachment faulting mylonitization were estimated from feldspar thermometry to be $535^\circ \pm 44^\circ\text{C}$ in deeper portions of the lower plate and $458^\circ \pm 35^\circ\text{C}$ in structurally higher portions such as Bowman's Wash (23). The highest oxygen isotope temperatures in the sample farthest from the fault (90-WP-14) are equivalent within uncertainty to ambient predetachment temperatures of $\sim 460^\circ\text{C}$ estimated from cation thermometry (Fig. 3). Toward the fault, mean oxygen isotope temperatures decreased 82°C over 38 m, or 2160°C per kilometer (Fig. 3). At distances of >50 m below the fault the geothermal gradient likely decreases to nominal values (23).

Conductive cooling alone cannot account for this gradient, which is one to two orders of magnitude greater than gradients typically produced by conductive cooling. Shear-induced mechanical juxtaposition of rocks from different thermal regimes is also not a likely cause of the gradient, because the footwall tonalite exhibits grain size reduction but not penetrative shearing and it is a continuous and coherent unit. The overlap in temperatures that adjacent sam-

ples show (Fig. 3) suggests that the timing and duration of fluid-rock interaction was broadly synchronous in all samples. We interpret the range of temperatures documented in each sample to reflect equilibration in discrete subvolumes of each sample as ambient temperatures decreased over a finite period of time. Thus, at any given depth lower temperatures are younger than higher temperatures. Because the lowest (youngest) temperature recorded in the sample farthest from the fault ($\sim 380^\circ\text{C}$) is essentially equivalent to the highest (oldest) temperature in the sample closest to the fault ($\sim 390^\circ\text{C}$), the range of temperatures in all samples was likely established during the same finite period of time. We thus interpret the gradient to document cooling of the footwall from ambient predetachment temperatures by means of advective removal of heat by fluids.

Thermal models indicate that for advective heat flow to occur high fluid fluxes and high permeabilities are necessary (24, 25), and both are characteristic of detachment faults. The cataclastic deformation associated with faulting (12, 19) would have significantly increased permeability below the fault surface. High fluid fluxes are indicated by the regional development of chloritic and silicified breccias and economically significant iron sulfide, cupric sulfide, and gold deposits.

For heat extraction to occur, the fluids must have been at low temperature relative to footwall rocks. Calculated $\delta^{18}\text{O}$ values of water in equilibrium with quartz range from 2.4 per mil just below the fault to 6.5 per mil at 50 m below the fault. As magmatic fluid should have $\delta^{18}\text{O}$ values of ~ 6 to 10 per mil, the fluids are unlikely to be igneous in origin. Instead, the range of fluid $\delta^{18}\text{O}$ values are more readily explained as surface-derived basin brines (26) or evolved meteoric waters. Thus, surface-derived fluids that are cold relative to footwall rocks are consistent with calculated fluid $\delta^{18}\text{O}$ values. The involvement of surface-derived fluids in detachment fault-related processes has been documented in a number of core

complexes (27–33).

Geochronologic and field studies indicate rapid upward transport of lower plate mylonites from below the brittle-ductile transition to near surface levels in <2 million years (12, 14, 34). Hornblende and muscovite $^{40}\text{Ar}/^{39}\text{Ar}$ ages from lower plate mylonites of 19.2 ± 0.2 and 18.0 ± 0.1 million years ago (Ma), respectively, indicate rapid cooling in the Whipple Mountains between ~ 19 and 18 Ma (14, 35). Cooling rates of $>50^\circ$ to 100°C per million years between ~ 19 and ~ 15 Ma from other cordilleran core complexes have been cited as evidence for rapid upward transport of the lower plate (15, 17).

Our data suggest instead that rapid cooling of lower plate rocks involved the influx of cold, surface-derived fluids that migrated down through the upper plate along high-angle normal faults. Thus, as lower plate rocks passed upward beneath these high-angle faults, they were infiltrated by cold, surface-derived fluids that effectively refrigerated the fault zone. Advective removal of heat from the footwall by fluids is also consistent with the absence of thermal metamorphic effects in upper plate rocks adjacent to the fault. Although uplift clearly remains an important element in the evolution of the core complex as mid-crustal rocks are exposed at the surface (34), our data indicate that rapid cooling in rocks affected by detachment fault-related processes reflects fluid infiltration.

Models assessing thermal aspects of crustal extension have generally considered only conductive cooling (15, 36). A recent study has suggested that the final stages of cooling in the Bucksin-Rawhide core complex may have been enhanced by fluid interaction (17). Our data, however, indicate that most of the cooling subsequent to mylonitization is the result of advective heat extraction by surface-derived fluids. Thermochronologic data, which provide the primary quantitative constraints on cooling and uplift rates associated with extension, document rapid Miocene cooling in many core complexes (12, 15, 17). If footwall refrigeration is a wide-

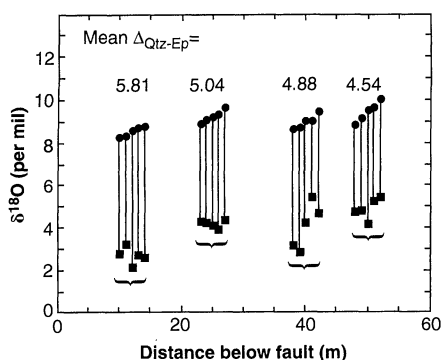
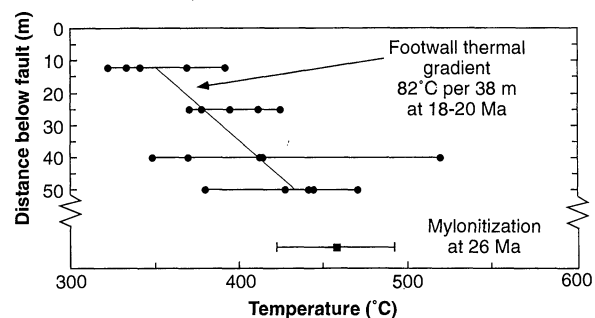


Fig. 2. Coexisting quartz (circles) and epidote (squares) $\delta^{18}\text{O}$ values plotted versus distance below the detachment fault. The five quartz-epidote pairs from each sample represent discrete subvolumes of the sample. For each sample, values are arbitrarily arranged in order of increasing quartz $\delta^{18}\text{O}$. The mean $\Delta_{\text{Qtz-Ep}}$ value decreases toward the fault from 4.54 ± 0.46 per mil to 5.81 ± 0.52 per mil.

Fig. 3. Plot of temperatures estimated from oxygen isotope compositions (circles) versus distance below the fault. Mylonitization or ambient predetachment faulting temperatures of $\sim 458^\circ \pm 35^\circ\text{C}$ (square) for these structural levels were estimated from two-feldspar thermometry (23). The mean thermal gradient of $\sim 82^\circ\text{C}$ per 38 m is interpreted to result from infiltration of cold, surface-derived fluids into the upper portions of the lower plate during detachment faulting. The thermal gradient is thought to decrease to nominal values at depths >50 m below the fault.



spread phenomenon, these studies may have overestimated the role of tectonic denudation as a cause of cooling. If rapid cooling reflects the infiltration of cold, surface-derived fluids, then cooling rates cannot be used to constrain uplift rates. Rather, the timing of rapid cooling reflects the transport of lower plate rocks into the zone of fluid infiltration. Thus, quantitative constraints on uplift rates associated with extensional detachment faults should be determined with the use of well-constrained field relations and pressure-temperature-time data based on thermobarometry and radiogenic age determinations.

REFERENCES AND NOTES

1. M. D. Crittenden, P. J. Coney, G. H. Davis, Eds., *Geol. Soc. Am. Mem.* **153** (1980).
2. B. Wernicke, *Nature* **291**, 645 (1981).
3. R. L. Armstrong, *Annu. Rev. Earth Planet. Sci.* **10**, 129 (1982).
4. B. Wernicke, *J. Geophys. Res.* **100**, 20159 (1995).
5. E. M. Anderson, *The Dynamics of Faulting* (Oliver and Boyd, Edinburgh, ed. 1, 1942).
6. J. A. Jackson, in *Continental Extensional Tectonics*, M. P. Coward, J. F. Dewey, P. L. Hancock, Eds. (Geological Society of London, Special Publ. 28, London, 1987), pp. 3–18.
7. W. R. Buck, *Tectonics* **7**, 959 (1988).
8. B. Wernicke, *Can. J. Earth Sci.* **22**, 108 (1985).
9. _____ and G. J. Axen, *Geology* **16**, 848 (1988).
10. W. R. Buck, F. Martinez, M. S. Steckler, J. R. Cochran, *Tectonics* **7**, 213 (1988).
11. A. Yin, *ibid.* **8**, 469 (1989).
12. G. A. Davis and G. S. Lister, *Geol. Soc. Am. Spec. Pap.* **218**, 133 (1988).
13. G. J. Axen, *J. Geophys. Res.* **97**, 8979 (1992).
14. R. K. Dokka and S. H. Lingrey, in *Cenozoic Paleogeography of the Western United States*, J. M. Armentrout et al., Eds. (Pacific Section of the Society of Economic Paleontologists and Mineralogists, Los Angeles, 1979), pp. 141–146.
15. D. A. Foster, T. M. Harrison, C. F. Miller, K. A. Howard, *J. Geophys. Res.* **95**, 20005 (1990).
16. D. K. Holm and R. K. Dokka, *Earth Planet. Sci. Lett.* **116**, 63 (1993).
17. R. J. Scott, D. A. Foster, G. S. Lister, *Geol. Soc. Am. Bull.*, in press.
18. R. K. Dokka, *Geology* **21**, 711 (1993).
19. G. A. Davis, J. L. Anderson, E. G. Frost, T. J. Shackelford, *Geol. Soc. Am. Mem.* **153**, 79 (1980).
20. We extracted oxygen from silicate minerals using the CO₂ laser-probe system [Z. D. Sharp, *Geochim. Cosmochim. Acta.* **54**, 1353 (1990)]. Silicate samples (~0.2 to ~1 mg) were loaded into individual wells 2 mm in diameter in a solid Ni sample holder and heated in the presence of BrF₅ with a 20-W CO₂ laser. The liberated O₂ gas was converted to CO₂ by reaction with hot graphite. The CO₂ gas was analyzed on a VG Prism gas-ratio mass spectrometer. Accuracy and precision were assessed by 26 analyses of the Gore Mountain garnet standard [J. W. Valley, N. Kitchen, M. J. Kohn, C. R. Niendorf, M. J. Spicuzza, *Geochim. Cosmochim. Acta.* **59**, 5223 (1996)], which yielded a mean value of 5.81 ± 0.16 per mil (accepted value, 5.8 per mil).
21. A. Matthews, *J. Metamorph. Geol.* **12**, 211 (1994).
22. R. T. Gregory and R. E. Criss, in *Stable Isotopes in High Temperature Geological Processes*, J. W. Valley, H. P. Taylor, J. R. O'Neil, Eds. [*Reviews in Mineralogy* **16**, Mineralogy Society of America, Washington, DC, 1986], p. 91.
23. J. L. Anderson, in *Metamorphic and Crustal Evolution of the Western United States*, W. G. Ernst, Ed. (Prentice-Hall, Englewood Cliffs, NJ, 1988), pp. 503–525.
24. M. J. Bickle and D. McKenzie, *Contrib. Mineral.*

Petrol. **95**, 384 (1987).

25. K. P. Furlong, R. B. Hanson, J. R. Bowers, in *Contact Metamorphism*, D. M. Kerrich, Ed. [*Reviews in Mineralogy* **26**, Mineralogy Society of America, Washington, DC, 1991], p. 437.
26. M. S. Roddy, S. J. Reynolds, B. M. Smith, J. Ruiz, *Geol. Soc. Am. Bull.* **100**, 1627 (1988).
27. J. E. Spencer and J. W. Welty, *Geology* **14**, 195 (1986); J. Wilkins, T. Heidrick, R. Beane, *Ariz. Geol. Soc. Dig.* **16**, 108 (1986).
28. S. J. Reynolds and G. S. Lister, *Geology* **15**, 362 (1987).
29. R. Kerrich and W. Rehrig, *ibid.*, p. 58.
30. R. D. Halfkenny, R. Kerrich, W. A. Rehrig, *Ariz. Geol. Surv. Bull.* **198**, 190 (1989).
31. B. M. Smith, S. J. Reynolds, H. W. Day, R. J. Bodnar, *Geol. Soc. Am. Bull.* **103**, 559 (1991).

32. J. Morrison, *J. Metamorph. Geol.* **12**, 827 (1994).

33. S. Losh, *Geol. Soc. Am. Bull.* **109**, 300 (1997).
34. J. L. Anderson, A. P. Barth, E. D. Young, *Geology* **16**, 366 (1988).
35. E. DeWitt, J. F. Sutter, G. A. Davis, J. L. Anderson, *Geol. Soc. Am. Abstr. Prog.* **118**, 584 (1986).
36. C. Ruppel, L. Royden, K. V. Hodges, *Tectonics* **7**, 947 (1988).
37. This research was supported by NSF grants EAR-91-05924, EAR-92-18953, and EAR-93-16651 to J.M. N. Kitchen provided invaluable assistance during this project. This manuscript was completed while J.M. was on sabbatical leave at the California Institute of Technology. We thank G. Davis, A. Yin, and two anonymous reviewers for helpful comments.

15 August 1997; accepted 11 November 1997

Suppression of Volcanism During Rapid Extension in the Basin and Range Province, United States

P. B. Gans* and W. A. Bohrsen

Continental extension and volcanism are generally thought to be complementary. Stratigraphic and structural data from some highly extended parts of the Basin and Range province reveal instead that rapid extension appears to have suppressed volcanism. This relation may reflect enhanced crystallization of midcrustal magmas during extension resulting from exsolution of magmatic volatiles, increased interaction of magmas with meteoric water, and dispersal of magma into smaller bodies. Some rift environments may thus be characterized by voluminous synextensional plutonism with little or no concomitant volcanism.

The Basin and Range province of western North America (Fig. 1) has been extended by 50 to 100% (200 to 300 km) and was the locus of voluminous mafic to silicic volcanism throughout the mid- to late Cenozoic (1). The relation between extension and volcanism in the province, however, is controversial (2, 3). In more highly extended domains, volcanism often preceded short-lived episodes of large-magnitude extension (3). Such a progression supports an active rifting model, wherein ascent of mantle-derived magmas triggers extensional collapse of the lithosphere (3). In a passive rifting model, stretching and thinning of lithosphere cause decompression melting in the asthenosphere, such that volcanism follows the onset of extension (4). Implicitly, the generation, ascent, and eruption of magma ought to be enhanced once extension is under way in both models. Here, we document the relation between extension rates and eruption rates in the northern Colorado River extensional corridor (CREC) in the Basin and Range province and show that rapid extension suppressed

rather than enhanced volcanic activity.

The CREC (5) is a 50- to 100-km-wide region of highly extended upper crust (Fig. 1), characterized by pervasive normal faulting and steep tilting of upper crustal sections. Both volcanism and rapid extension migrated northward from near the Whipple Mountains at 22 to 17 million years ago (Ma) to near Las Vegas, Nevada, at 14 to 12 Ma (6, 7), but the inception and peak of volcanism typically predate the peak of extension (3). This relation is best documented in the Eldorado Mountains (8) (Figs. 2 and 3). Volcanic rocks here include the following: 18.5- to 15.1-Ma trachyandesite to dacite lavas and breccias, a 15.1-Ma dacite ignimbrite, 15.1- to 14.1-Ma basalt and trachydacite flows intercalated with coarse clastic debris, and 14.1- to 13.0-Ma capping basalts and trachyandesites that unconformably overlie the older rocks (Fig. 2). The Eldorado Mountains represent a major eruptive center (8), and the entire 4-km-thick volcanic section is locally derived. Average volcanic accumulation rates increased from less than 1 mm/year at 17 Ma to a peak of 3 mm/year between 15.8 and 15.0 Ma, and then abruptly dropped at 15.0 Ma (Fig. 3A). Volcanic activity resumed after 14.2 Ma, but average accumulation rates were slower by an order of magnitude (~0.3 mm/year).

Department of Geological Sciences and Institute for Crustal Studies, University of California, Santa Barbara, CA 93106, USA.

*To whom correspondence should be addressed. E-mail: gans@magic.geol.ucsb.edu